INTERNATIONAL JOURNAL OF CLIMATOLOGY
Int. J. Climatol. **27**: 531–540 (2007)
Published online 25 September 2006 in Wiley InterScience
(www.interscience.wiley.com) DOI: 10.1002/joc.1417

RMetS
ROYAL METEOROLOGICAL SOCIETY

Relations of South American summer rainfall interannual variations with the Pacific Decadal Oscillation

Mary T. Kayano* and Rita V. Andreoli
Instituto Nacional de Pesquisas Espaciais, Centro de Previsão de Tempo e Estudos Climáticos, Avenida dos Astronautas, 1758, 12227-010 São José dos Campos, SP, Brazil

Abstract:

The anomaly patterns of rainfall in South America for El Niño/Southern Oscillation (ENSO) extreme conditions stratified according to the high, low, and normal Pacific (inter-) Decadal Oscillation (PDO) phases (HPDO, LPDO and NPDO) are examined for the three bi-months of the season from November to April. El Niño (EN) and La Niña (LN) composites as well as the linear (EN − LN) and nonlinear (EN + LN) components of the precipitation anomaly patterns relative to ENSO show substantial differences among the three PDO phases. The differences in the strength of ENSO teleconnections for the South American rainfall might be related to the PDO, which creates a background for these teleconnections acting constructively (destructively) when ENSO and PDO are in the same (opposite) phase. An interesting aspect is the occurrence of robust structures of the nonlinear component, which are due to the same sign rainfall anomalies for EN and LN composites. This is particularly conspicuous for the HPDO over eastern Brazil in the South Atlantic Convergence Zone (SACZ) region during Nov/Dec and Jan/Feb, for the HPDO over northern/northwestern South America during Mar/Apr, and for the NPDO over northeastern Brazil during Mar/Apr. The results presented here might have relevant implications for climate monitoring purposes.

KEY WORDS El Niño/Southern Oscillation; Pacific Decadal Oscillation; rainfall; climate variability

Received 19 October 2005; Revised 20 July 2006; Accepted 23 July 2006

INTRODUCTION

The major source of interannual climate variations in several parts of the globe is the El Niño/Southern Oscillation (ENSO) phenomenon. The ENSO modus operandi comprises the El Niño (EN) in one extreme phase (warm phase) and the La Niña (LN) in the opposite extreme (cold phase). The EN-related coupled atmospheric–oceanic characteristics show above-normal sea-level pressure (SLP) over Indonesia, and below-normal SLP in the central and eastern tropical Pacific associated with an abnormally eastward displaced Walker circulation with the descending branch in the western equatorial Pacific and the ascending branch in the central and eastern equatorial Pacific, where above-normal sea-surface temperature (SST) prevails. These features are accompanied by weakened low-level equatorial Pacific easterlies and by enhanced convection in the central and eastern tropical Pacific; there, a pair of anomalous upper tropospheric anticyclonic centers on both sides of the equator at low latitudes is established (Rasmusson and Arkin, 1985). LN events generally feature reversed atmospheric and oceanic patterns (Kousky and Ropelewski, 1989).

The ENSO cycle explains a large part of the interannual rainfall variability in South America (Walker, 1928; Caviedes, 1973; Hastenrath and Heller, 1977; Kousky *et al*., 1984; Ropelewski and Halpert, 1987, 1989, hereafter RH87 and RH89; Aceituno, 1988; Kayano *et al*., 1988; Kiladis and Diaz, 1989; Rao and Hada, 1990; Barros and Silvestri, 2002; Grimm, 2003; Kayano, 2003; Vera *et al*., 2004). This variability is more pronounced in two areas: (1) the Northeast (French Guiana, Venezuela, Guyana, Surinam, and near equatorial regions of Brazil), and (2) the Southeast (southern Brazil, Uruguay, and parts of northern Argentina) (RH87, RH89). The anomalous conditions in these areas show seasonal differences, with dry (wet) conditions in the Northeast during July–March (June–March), and wet (dry) conditions in the Southeast during November–February (June–December) for EN (LN) episodes (RH87, RH89). The first month of these periods refers to the onset year of ENSO extremes.

Moreover, recent studies provided diagnostic evidence on modulations of ENSO teleconnections by lower frequency climate modes (Gershunov and Barnett, 1998; McCabe and Dettinger, 1999; Gutzler *et al*., 2002; Krishnan and Sugi, 2003; Brown and Comrie, 2004; Chelliah and Bell, 2004; Andreoli and Kayano, 2005). One of these modes is the so-called Pacific (inter-) Decadal Oscillation (PDO), which is part of the

* Correspondence to: Mary T. Kayano, Instituto Nacional de Pesquisas Espaciais, Centro de Previsão de Tempo e Estudos Climáticos, Avenida dos Astronautas, 1758, 12227-010 São José dos Campos, SP, Brazil; e-mail: mary@cptec.inpe.br

decadal–multidecadal variability in the tropical and midlatitude Pacific (Mantua *et al*., 1997). Although the PDO signs are prominent in the North Pacific, the anomaly patterns of SST, SLP, and surface wind stress fields in the Pacific for this mode are quite similar to the corresponding patterns for the ENSO mode (Mantua *et al*., 1997; Zhang *et al*., 1997; Garreaud and Battisti, 1999; Mestas-Nuñez and Enfield, 2001; Chelliah and Bell, 2004). The PDO anomaly pattern for SST is nearly symmetric relative to the equator, but is less equatorially confined in the eastern Pacific than that of the ENSO mode (e.g. Zhang *et al*., 1997; Zhang *et al*., 1998; Enfield and Mestas-Nuñez, 1999). Minobe (2000) found the most energetic PDO fluctuations in two periodicities: 15–25 years and 50–70 years. Mantua *et al*. (1997), using SST and SLP data, found the PDO-related reversals in the polarity of the oscillations with the 50–70 years periodicity. They found that the cold PDO regime occurred during the 1900–1924 and 1947–1976 periods, while the warm PDO regime occurred during the 1925–1946 period, and from 1977 to the middle of the 1990s. They also showed that the warm PDO regime features an abnormally deep Aleutian low-pressure system, negative SST anomalies in the western and central North Pacific, and positive SST anomalies along the west coast of the Americas and in the central and eastern tropical Pacific. The cold PDO regime features nearly reversed patterns.

Although decadal and long-term trend variations have been detected for hydrometeorological parameters in South America (Dias de Paiva and Clarke, 1995; Marengo *et al*., 1998; Krepper and Sequeira, 1998; Robertson and Mechoso, 1998, 2000; Zhou and Lau, 2001; Paegle and Mo, 2002), only more recently have these variations been interpreted in the context of the PDO effects (Chelliah and Bell, 2004; Marengo, 2004; Kayano and Andreoli, 2004; Andreoli and Kayano, 2005). Marengo (2004) noted decadal shifts in the northern Amazon rainfall regime consistent with the PDO shifts of 1946–1947 and 1976–1977. Marengo (2004) found less rainfall after 1975 than before in the northern Amazon. In a more comprehensive analysis on the multidecadal climate variability in the tropics, Chelliah and Bell (2004) found strong EN (LN) teleconnections for the warm (cold) PDO regime. Using composites of the rainfall anomalies over South America for warm and cold PDO regimes, Andreoli and Kayano (2005) found consistent results.

These studies consider that the PDO regimes are continuous epochs with approximately a 20–30 year of duration, without breakdowns within each epoch. However, some breakdowns are observed within the PDO regimes. In order to take these breakdowns into account, three PDO phases are considered: high, normal, and low. It seems that the knowledge about the relationship of PDO phases and strength of ENSO effects for individual years may have a potential use in improving climate monitoring. Therefore, ENSO-related anomaly patterns of rainfall over South America, taking the PDO phases for individual years into account, are investigated here. Analyses are done for the warm season (from November to April) because a large portion of South America presents its principal rainy regime during this season (Rao and Hada, 1990; Rao *et al*., 2002) and ENSO teleconnections are strong in both hemispheres during this season (Kayano and Andreoli, 1998).

DATA AND METHODOLOGY

The data used in this paper consists of the reconstructed monthly gridded SST data (version 2 SST data) of 1854–2000 at a 2° by 2° latitude–longitude resolution (Smith and Reynolds, 2003). Precipitation data over South America during 1912–1998 is extracted from a historical monthly precipitation data set for global land areas gridded at a 2.5° by 3.75° latitude–longitude resolution grid available for the 1900–1998 period. This data set is obtained from Dr Mike Hulme's Web page (http://www.cru.uea.ac.uk/~mikeh/datasets/global) at the Climatic Research Unit, University of East Anglia, Norwich, UK. Description of this data set can be found in Hulme (1992, 1994) and in Hulme *et al*. (1998). A total of 105 grid points in the South American sector between 10 °N and 40 °S, whose locations are illustrated in Figure 1, are used here. The base period of analysis is from 1912 to 1998. Monthly precipitation anomalies at each grid point are obtained as departures from the 1912–1998 means. The anomaly series at each grid point are standardized by the corresponding standard deviation of the anomaly time series.

The PDO index during 1900–2003 is obtained from the Web page address at ://ftp.atmos.washington.edu/mantua/pnw_impacts/INDICES/PDO.latest. A seasonal PDO index is obtained by averaging the monthly values from October to March. The Niño 3.4 SST index, defined as the 5-month running mean of the averaged SST anomalies in the area bounded by 4 °N, 4 °S, 170 °W, and 120 °W, is obtained for the 1855–1999 period. In order to avoid biases due to the PDO regimes, the SST anomalies used in the computation of the Niño 3.4 SST index are departures from the 1854–2000 means. A seasonal Niño 3.4 SST index is calculated averaging the monthly values

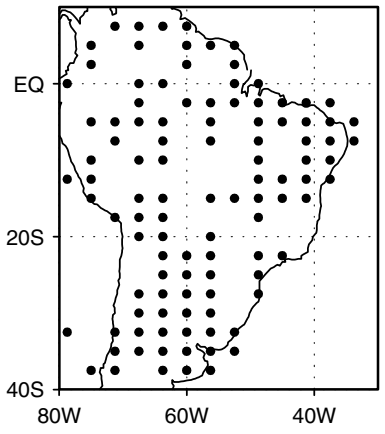

Figure 1. Locations of the rainfall grid points

DOI: 10.1002/joc

Table I. El Niño (EN) and La Niña (LN) years according to the PDO phases

	LPDO	NPDO	HPDO
LN	1916, 1917, 1949, 1950, 1955, 1962, 1967, 1970, 1973, 1975, 1988, 1998	1915, 1920, 1922, 1924, 1928, 1931, 1933, 1937, 1942, 1944, 1954	1926, 1934, 1936, 1938, 1984, 1995
EN	1951, 1953, 1963, 1965, 1968, 1990, 1994	1913, 1914, 1957, 1958, 1972, 1977, 1991	1923, 1925, 1930, 1939, 1940, 1941, 1969, 1976, 1979, 1982, 1986, 1987, 1992, 1997

from December to February. Following the suggestions on Dr. Mantua's Web page, 0.5 standard deviations of the seasonal PDO and Niño 3.4 SST indices, of the 0.43 °C and 0.46 °C, respectively, are the threshold to identify the PDO and ENSO phases. Therefore, seasonal PDO indexes less than −0.43 °C, between −0.43 °C and 0.43 °C, and greater than 0.43 °C classify the years as having low, normal, and high PDO (LPDO, NPDO, and HPDO) phases, respectively. Similarly, the LN and EN years are those with seasonal Niño 3.4 SST indexes less than −0.46 °C and greater than 0.46 °C, respectively. Table I lists the ENSO extremes of the 1912–1998 period classified according to the PDO phases. Since seasonal indices are used, the years listed in Table I refer to the year of the first month of the seasons.

Composites are prepared for the bi-months, November–December (Nov–Dec), of the years listed for each case in Table I and for the bi-months, January–February (Jan–Feb) and March–April (Mar/Apr), of the following years. This temporal stratification is justified because the southeastern South America rainfall anomalies show the strongest (weakest) relationship with the SST anomalies in the tropical and subtropical Atlantic and eastern Pacific Oceans during Nov/Dec (Jan/Feb) (Berri and Bertossa, 2004). Further, these bi-months overlap the periods identified by RH87 (RH89) with EN (LN) coherent signals for the precipitation in the northeastern and southeastern tropical South America.

The linear (nonlinear) components of the climate response to ENSO extremes are estimated by the difference between (summation of the) EN and LN composites (Hoerling *et al*., 1997). So, EN, LN, EN − LN, and EN + LN composites are obtained for the three PDO phases. In order to assess the statistical significance of the EN, LN, and EN + LN composites, the number of degrees of freedom is taken as the number of events. For these composites, it is assumed that a variable X with n values and S standard deviation has a Student-t distribution. So, only the composites (indicated by $\overline{X}$) with absolute values exceeding $t_{\alpha(n-2)}S/\sqrt{(n-2)}$ are statistically significant (Panofsky and Brier, 1968). For the EN − LN composites, X_1 and X_2 being the variables for EN and LN events with n_1 and n_2 values, S_1 and S_2 standard deviations, and their composites indicated by $\overline{X_1}$ and $\overline{X_2}$, respectively, it is assumed that the difference $X_1 - X_2$ has a Student-t distribution. Only the absolute values of $\overline{X_1} - \overline{X_2}$ exceeding $t_{\alpha(n1+n2-2)}\sqrt{(n_1-1){S_1}^2 + (n_2-1){S_2}^2}\sqrt{\dfrac{n_1+n_2}{n_1n_2(n_1+n_2-2)}}$ are statistically significant for the confidence level of 95% (Press *et al*., 1986).

RESULTS

Indices

Figure 2 shows the seasonal PDO (continuous curve) and Niño 3.4 SST (dashed curve) indices, EN (open circle) and LN (asterisk) years. The seasonal PDO and Niño 3.4 SST indices show synchronized fluctuations with different amplitudes during some periods and opposite fluctuations during others. Indeed, the positive correlation (0.38) between the two indices for the 1912–1999 period is highly significant (Table II). The value of the correlation coefficient increases when it is calculated for the 1947–1976 period. All correlation coefficients in Table II are significant at 90% confidence level by Student's t-test. Correlations between the two indices for the 1912–1999 and 1947–1976 periods are significant at the 99.9% confidence level.

The breakdowns in the PDO index define the HPDO, LPDO, and NPDO phases. Indeed, this index is predominantly less than −0.43 °C (>0.43 °C) during the cold (warm) PDO periods of 1912–1924 and 1947–1976 (1925–1946 and 1977–1999) but with the occurrences

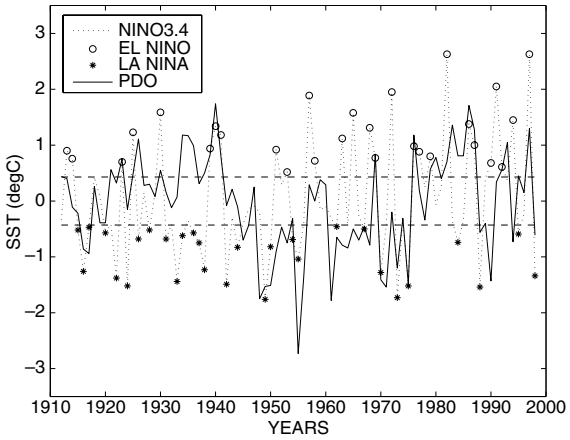

Figure 2. Seasonal PDO (continuous curve) and Niño 3.4 SST (dashed curve) indices. The horizontal dashed lines are the threshold of PDO index at −0.43 °C and 0.43 °C. Open circles and asterisks indicate EN and LN years

DOI: 10.1002/joc

Table II. Correlation coefficients (c.c) between seasonal PDO and Niño 3.4 SST indices

Period	1912–1999	1925–1946	1947–1976	1977–1999
c.c	0.38	0.36	0.55	0.37

of some values greater (less) than −0.43 °C (0.43 °C). So, during the warm (cold) PDO regime, the PDO index dominantly features HPDO (LPDO) phases and secondly LPDO (HPDO) and NPDO phases. This is evident in Figure 2.

HPDO composites

The mean rainfall anomaly patterns for EN years of the HPDO phase during Nov/Dec, Jan/Feb, and Mar/Apr are shown in Figure 3(a). The pattern during Nov/Dec shows positive anomalies in the coast of northern Peru and Ecuador and in southeastern South America (northeastern Argentina, Uruguay, southern and

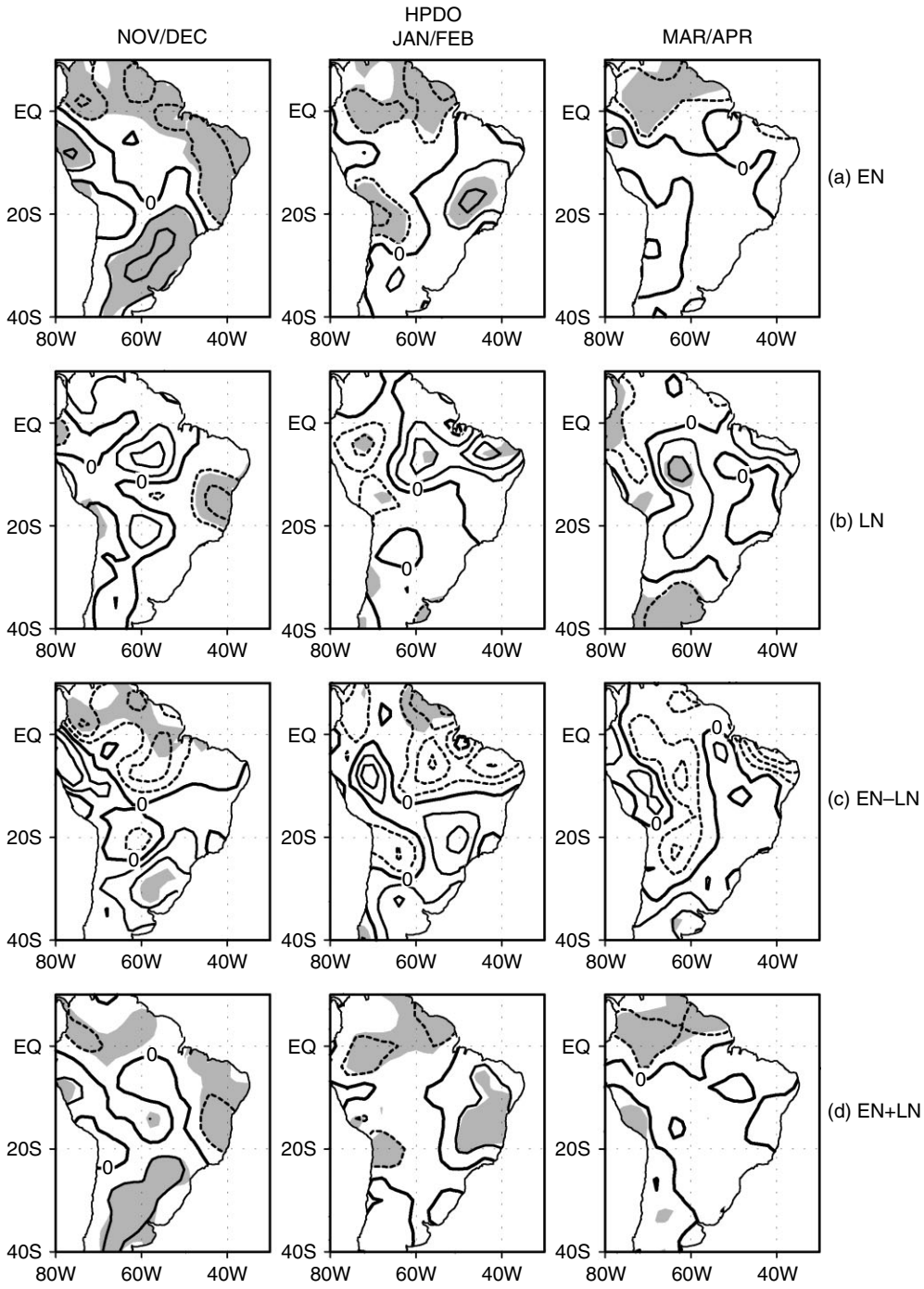

Figure 3. Mean standardized rainfall anomalies for the HPDO phase during Nov/Dec, Jan/Feb, and Mar/Apr of: (a) EN years; (b) LN years; (c) EN − LN composites, and (d) EN + LN composites. Contour interval is 0.3 standard deviations, with negative (positive) contours being dashed (continuous). Shaded areas encompass significant values at the 95% confidence level

DOI: 10.1002/joc

southeastern Brazil), negative anomalies over northern, northwestern, and northeastern South America, and hints of negative anomalies over the central Andes (Altiplano). The spatially prominent patterns with negative anomalies over northwestern/northern/northeastern South America and positive ones over southeastern South America show correspondence with the EN-related rainfall anomaly patterns for November and December obtained by Paegle and Mo (2002) (their Figure 5(e) and (f)). In Jan/Feb, the positive anomalies weaken considerably, the negative ones remain over northwestern and northern South America, the negative anomalies over northeastern Brazil are replaced by weak positive anomalies with significant values centered approximately at (15 °S, 45 °W), and the negative anomalies over the Altiplano intensify. In Mar/Apr, the significant negative anomalies remain over northwestern and northern South America, while relatively small anomalies are found elsewhere.

The EN-related anomalous east–west circulation with ascending motion over eastern Pacific and descending motion over the Atlantic and adjacent South American continental areas might be responsible for positive anomalies in the coast of northern Peru and Ecuador and reduced precipitation over northeastern South America during Nov/Dec. The above-normal rainfall observed in eastern South America centered approximately at (15 °S, 45 °W) during Jan/Feb is, in part, explained by the presence of positive SST anomalies in the equatorial and tropical South Atlantic noted for the associated SST anomaly composite (Figure not shown). In this case, warmer than normal surface waters in the equatorial and tropical South Atlantic might enhance the actions of synoptic phenomena such as slow moving cold fronts and subtropical upper tropospheric cyclonic vortices. These systems play an important role in modulating the rainfall in eastern and northeastern Brazil during the austral spring, summer, and fall seasons (Kousky, 1979; Kousky and Gan, 1981). The EN-related upper level anticyclone over southeastern South America for warm PDO regime (Andreoli and Kayano, 2005) explains the above-normal rainfall noted in this region during Nov/Dec. The negative rainfall anomalies over the Altiplano during Jan/Feb might be related to the EN-related warming of the tropical troposphere and the associated strengthening of upper level westerlies over central Andes, as proposed by Garreaud and Aceituno (2001).

The LN composites of rainfall for the HPDO phase shows quite a different evolution and a smaller magnitude of the anomalies, which are nonsignificant in most of the South American region (Figure 3(b)). So, the combined effects of LN and HPDO on the rainfall in this region are relatively weak. Negative anomalies with small magnitudes are found along the eastern sector of the continent, over Ecuador and northern Peru, and positive ones are found elsewhere in tropical South America during Nov/Dec. This pattern evolves into an LN-related configuration, with hints of positive rainfall anomalies over a large area extending from the central and eastern Amazon towards central and northeastern Brazil and negative ones in most of western and southeastern South America, in particular over Ecuador and northern Peru, during Jan/Feb. In Mar/Apr, an LN-related pattern is established with significant negative rainfall anomalies over southeastern South America, Ecuador, and northern Peru, and positive anomalies over central and northeastern South America.

Owing to the small magnitudes of the rainfall anomalies for LN composites, the linear component of ENSO effect on the South American rainfall shows significant values only in given areas (Figure 3(c)). The EN − LN composite for Nov/Dec shows significant positive values in southeastern South America and negative ones over northern/northwestern South America. In Jan/Feb, negative EN − LN values are found in most of the area to the north of 10 °S and positive ones to the south of this latitude, except over southwestern Bolivia. In Mar/Apr, the EN − LN values are nonsignificant everywhere in the study domain.

The nonlinear component of ENSO-related precipitation composite is shown in Figure 3(d). In some cases, the significant EN + LN values reflect the unbalanced magnitudes of opposite sign EN- and LN-related rainfall anomalies. This is the case of the positive EN + LN values over southeastern South America and of the negative ones over northwestern South America during Nov/Dec, over northern South America (between 60 °W and 50 °W) during Jan/Feb, and over northeastern coast of South America during Mar/Apr. However, it is interesting to note that significant EN + LN values in some cases result from the same sign rainfall anomalies for EN and LN composites. This occurs over eastern Brazil (between 10 °S and 20 °S), where significant EN + LN values during Nov/Dec (negative) and during Jan/Feb (positive) are noted. This area is included among those where summer rainfall variability is affected by the South Atlantic Convergence Zone (SACZ), a quasi-stationary northwest–southeast oriented cloud band over South America (Streten, 1973; Yasunari, 1977; Kodama, 1992, 1993), which is part of the South American monsoon system (Grimm *et al.*, 2004). So the nonlinear component of precipitation composite over eastern Brazil, in part, reflects the effects of the SACZ-related cold fronts, which in some cases are related to the presence of subtropical upper tropospheric cyclonic vortices (Kousky and Gan, 1981).

Significant negative EN + LN values resulting from the same sign rainfall anomalies for EN and LN composites are also noted over northern/northwestern South America during Mar/Apr. ENSO-coherent interannual precipitation variations have been previously documented over northern South America with negative anomalies during EN years and positive ones during LN years (Ropelewski and Halpert, 1987, 1989; Kousky and Ropelewski, 1989). The composites here show negative rainfall anomalies in this region for both EN and LN years

DOI: 10.1002/joc

during Mar/Apr (Figure 3(a) and (b)). However, the negative anomalies for the LN composite show quite small magnitudes compared to those for the EN composite. In consequence, the negative EN + LN values over northern/northwestern South America during Mar/Apr reflect mostly the EN-related anomalies (Figure 3(a), (b) and (d)). Although weak, negative rainfall anomalies are not expected over northern South America during Mar/Apr of LN years (Ropelewski and Halpert, 1989). So, other factors influence the rainfall variations over northern South America during Mar/Apr of the LN years included in the present analysis.

LPDO composites

The EN composite of rainfall for the LPDO phase features negative anomalies with small magnitudes over northern/northwestern South America, and over southeastern, central and most of northeastern Brazil and positive ones in the remaining areas, with significant values confined to central eastern Argentina during Nov/Dec (Figure 4(a)). In Jan/Feb, below-normal rainfall is noted in the area to the north of 20 °S and west of 60 °W and in southern South America between 25 °S and 40 °S, and hints of above-normal rainfall elsewhere, except

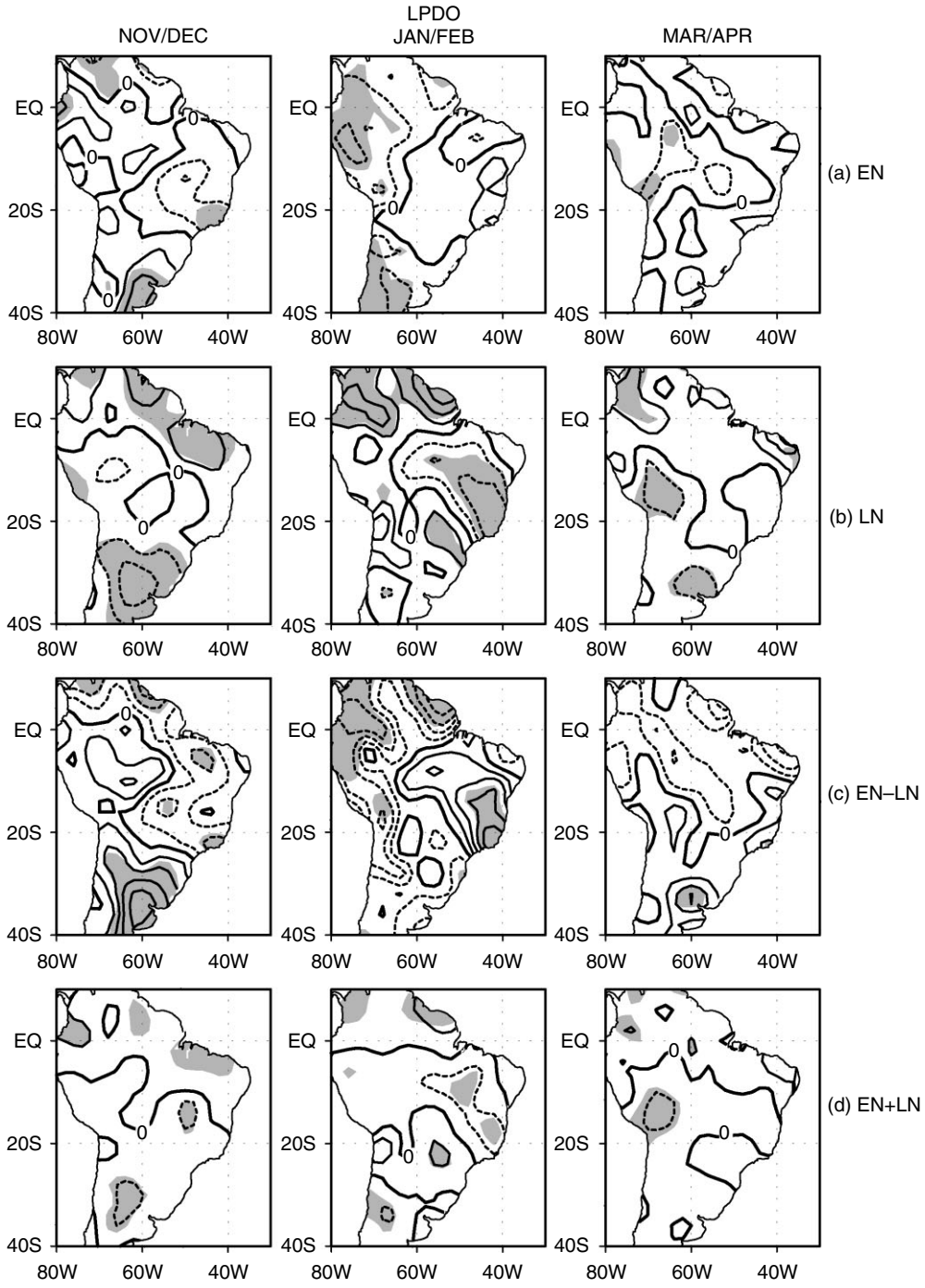

Figure 4. Same as in Figure 3, except for the LPDO phase

DOI: 10.1002/joc

over northeastern Brazil. For this bi-month, the significant anomalies are confined to northern Peru, Ecuador, and southwestern South America to the north of 40 °S (Figure 4(a)). In Mar/Apr, the rainfall anomalies are considerably smaller in most of the study domain.

The LN composite of rainfall shows above-normal rainfall in northwestern and northern South America and eastern Brazil, and below-normal rainfall in the remaining area of the study domain during Nov/Dec (Figure 4(b)). For this bi-month, significant positive rainfall anomalies are found over eastern Venezuela, Guyana, Surinam, and northern Brazil (northern Pará, Maranhão and Piauí States). The negative ones over central and northern Argentina, Uruguay, and southern Brazil are centered at 35 °S, 60 °W. When comparing this pattern with the LN-related rainfall anomaly composites over South America during November and December, as obtained by Paegle and Mo (2002) (their Figure 5(b) and (c)), the similarities are evident. However, the negative anomalies over southeastern South America for the present analysis are centered 5° to the south of those in their Figures. The significant positive rainfall anomalies in northern South America enhance and expand northwestward, occupying a large area from the mouth of the Amazon River to western Colombia and northern Ecuador during Jan/Feb. Most of the negative anomalies in central, western, and southeastern South America are replaced by small positive anomalies with significant values centered at 25 °S,

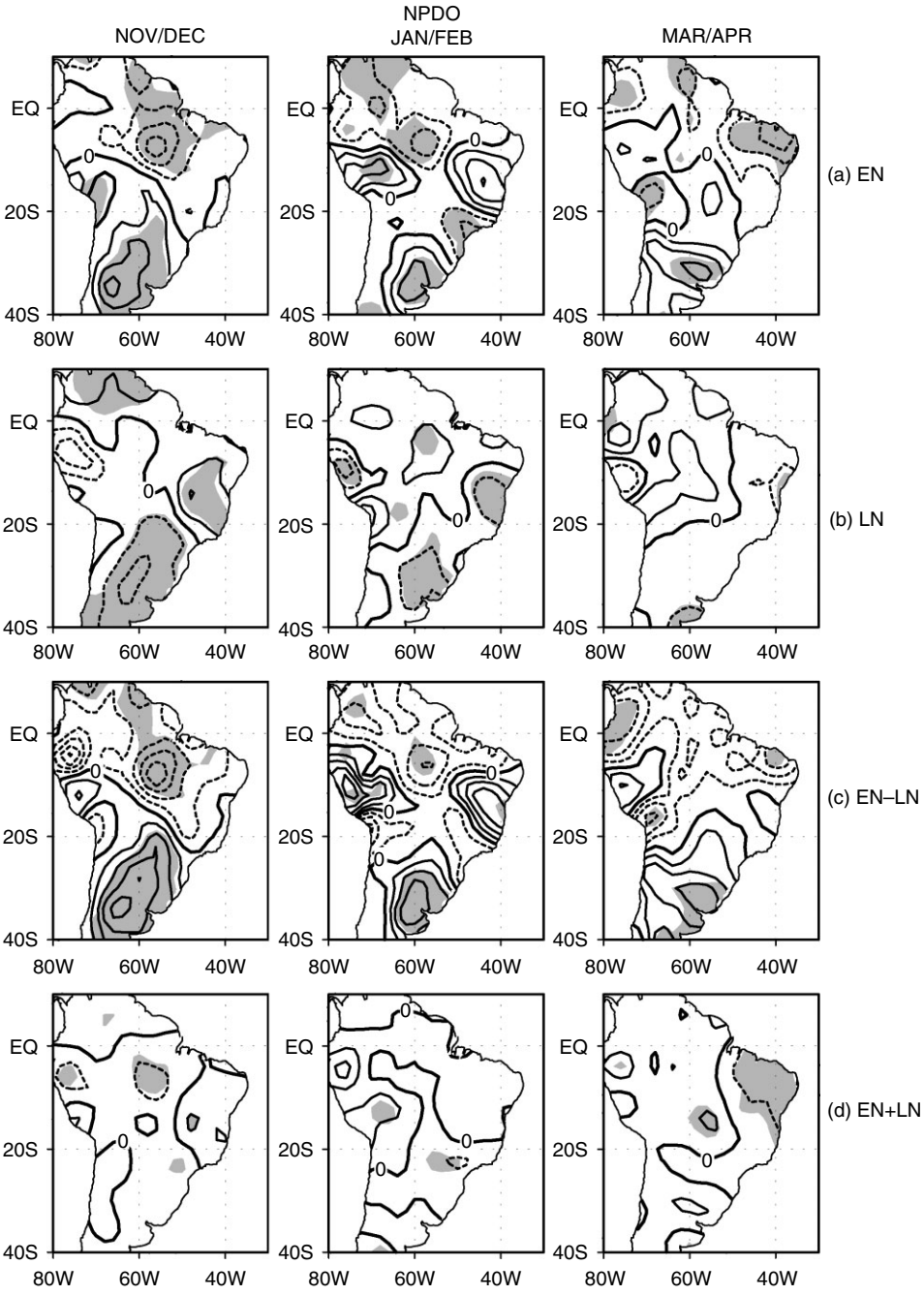

Figure 5. Same as in Figure 3, except for the NPDO phase

DOI: 10.1002/joc

55 °S during Jan/Feb (Figure 4(b)). In this bi-month, significant negative anomalies occupy an extensive area of eastern Brazil, approximately between 5 °S and 22 °S. This area coincides with the continental location of the SACZ. In Mar/Apr, the rainfall anomaly pattern features negative anomalies over western and southern sectors of the study domain, with significant values over Bolivia and Uruguay and positive anomalies in most of the remaining areas. For this bi-month, positive anomalies up to 0.3 standard deviations are also noted over the western equatorial lands and over the northeastern corner of the continent.

The linear component of the ENSO effect on the South American rainfall shows significant values over relatively extensive and well-defined areas during Nov/Dec and Jan/Feb (Figure 4(c)). Indeed, the EN − LN precipitation composite during Nov/Dec shows significant positive values over an extensive area of southeastern South America and in small areas to the north of the equator, and in the South American sector to the west of 60 °W and to the north of 25 °S. Significant negative EN − LN values are noted over northwestern and northern South America, and positive ones over southeastern Brazil in the SACZ region during Jan/Feb. In Mar/Apr, significant positive EN − LN values are noted only in a small area of southeastern South America.

For the LPDO, the significant EN + LN values are found in small areas scattered over the study domain and reflect mostly the unbalanced magnitudes of opposite sign EN- and LN-related rainfall anomalies (Figure 4(d)).

NPDO composites

The EN composite of rainfall for the NPDO phase shows significant positive anomalies in central and northeastern Argentina, Paraguay, Uruguay, and southern Brazil and negative ones centered in the eastern Amazon during Nov/Dec (Figure 5(a)). This composite evolves into a pattern with above-normal rainfall in a small area centered at 35 °S, 60 °W in central Peru, and below-normal rainfall in northwestern South America, southeastern Amazon, and southeastern Brazil during Jan/Feb (Figure 5(a)). In Jan/Feb, small positive rainfall anomalies are also noted in the southeastern continental edge of the SACZ. Finally, the EN composite features significant positive rainfall anomalies over Uruguay and negative ones over small areas to the north of equator, over northeastern Brazil, and the Altiplano during Mar/Apr. The rainfall deficits noted during Mar/Apr are in agreement with previous findings on EN effects on the South American rainfall (Aceituno, 1988; Kayano *et al*., 1988; Kiladis and Diaz, 1989; Rao and Hada, 1990).

The LN composite of rainfall for NPDO features negative anomalies in an extensive area of southeastern South America, including central and northeastern Argentina, Paraguay, Uruguay, and southern and southeastern Brazil, during Nov/Dec (Figure 5(b)). This composite also shows positive anomalies over northern Venezuela and Colombia and over the southeastern side of the SACZ over the continent. In Jan/Feb, the negative rainfall anomalies in southeastern South America and the positive ones over northern South America weaken considerably (Figure 5(b)). For this bi-month, significant negative anomalies are also observed over central western Peru and in the southeastern continental edge of the SACZ. In Mar/Apr, the LN-related rainfall anomalies show considerably small magnitudes with positive values in most of the South American sector to the north of 20 °S and west of 50 °W, and negative values elsewhere.

The linear component of ENSO effect on the South American rainfall for NPDO in general is relatively strong compared to those in the corresponding maps for HPDO and LPDO phases, in particular, in southeastern South America. In Nov/Dec, significant positive EN − LN values are found over the region south of 20 °S, and negative ones over the eastern Amazon (Figure 5(c)). In Jan/Feb, the significant EN − LN values are found over northeastern Argentina, Uruguay, and central Peru (positive), and over southeastern Amazon (negative). In Mar/Apr, positive EN − LN values are found to the south of 20 °S, with significant values over Uruguay, and negative ones in most of the remaining area of the study domain, with significant values over western Colombia and the northeastern corner of Brazil.

For the NPDO, the significant EN + LN values are found in small areas of the study domain during Nov/Dec and Jan/Feb bi-months (Figure 5(d)). In Mar/Apr, the significant negative EN + LN values over northeastern Brazil are due to the same sign (negative) rainfall anomalies in this region for the EN and LN composites. However, it is interesting to note that the significant negative EN + LN values over northeastern Brazil reflect mostly the negative EN-related anomalies. In this region, the negative LN-related anomalies show quite small magnitudes compared to those for the EN composite. However, negative rainfall anomalies are not expected over northeastern Brazil during Mar/Apr of LN years (Ropelewski and Halpert, 1989). So, other factors influence the rainfall over northeastern Brazil during Mar/Apr of the LN years analyzed here.

CONCLUSIONS

The relationship of the rainfall variability over South America and the ENSO is reexamined taking into account the high, normal, and low phases of the PDO (HPDO, LPDO, and NPDO) for the 1912–1998 base period. These phases are identified using the threshold of 0.43 °C for the seasonal (October to March) PDO index.

The El Niño (EN), La Niña (LN), EN − LN, and EN + LN composites show substantial differences among the PDO phases. ENSO teleconnections for the South American rainfall are considerably strong (weak) when ENSO and PDO are in the same (opposite) phases (Figures 3(a), (b) and 4(a), (b)). On the other hand, the opposite sign of the EN- and LN-related rainfall anomalies for the NPDO phase show comparable magnitudes

DOI: 10.1002/joc

(Figure 5(a), (b)). These results suggest that the differences in the strength of ENSO teleconnections are related to the PDO, which creates a background for these teleconnections to act constructively (destructively) when ENSO and PDO are in the same (opposite) phase.

An interesting result concerns the linear and nonlinear components of the rainfall response to ENSO extremes. These components show differences among the PDO phases. The linear (nonlinear) component of the ENSO-related precipitation anomaly patterns shows significant values in relatively large well-defined areas (small areas) for the LPDO and NPDO composites. Conversely, the linear (nonlinear) component of the ENSO-related precipitation anomaly patterns shows significant values in small (large) areas for the HPDO. However, the present analysis does not provide indications to explain why the nonlinear component of the ENSO-related precipitation is strong only for the HPDO phase.

Another interesting aspect is that the quite robust nonlinear structures for the HPDO and for the NPDO are due to the same sign rainfall anomalies for the EN and LN composites for some areas and bi-months. This is particularly conspicuous for the HPDO over eastern Brazil in the SACZ region during Nov/Dec and Jan/Feb, for the HPDO over northern/northwestern South America during Mar/Apr, and for the NPDO over northeastern Brazil during Mar/Apr. The negative EN + LN values during Mar/Apr for the HPDO over northern/northwestern South America, and for the NPDO over northeastern Brazil reflect mostly the negative precipitation anomalies of the corresponding EN composites, because the negative precipitation anomalies of the corresponding LN composites show quite small magnitudes in these regions. Although weak, negative rainfall anomalies are not expected over northern and northeastern South America during Mar/Apr of LN years (Ropelewski and Halpert, 1989). The result here indicates that other factors influence the rainfall in these regions during Mar/Apr of the LN years included in the analysis. In the case of northeast Brazil rainfall interannual variability, previous papers showed that in some situations the tropical Atlantic SST variability plays a more important role than the tropical Pacific SST variability (Giannini *et al*., 2004; Pezzi and Cavalcanti, 2001; Andreoli and Kayano, 2006).

The results presented here suggest that the traditional ENSO-based approach of climate monitoring would be improved if the information on the PDO phases were added. However, it is important to note that the results presented here refer to the combined PDO and ENSO effects as a result of the method used.

ACKNOWLEDGEMENTS

The authors are grateful to the two anonymous reviewers for their useful comments. The authors were partially supported by the Conselho Nacional de Desenvolvimento Científico e Tecnológico of Brazil. Thanks are also due to Dr. Mike Hulme for the provision of the 'gu23wld0098.dat' (version 1.0) constructed at the Climatic Research Unit, University of East Anglia, Norwich, UK.

REFERENCES

Aceituno P. 1988. On the functioning of the southern oscillation in the South American sector. Part 1: surface climate. *Monthly Weather Review* **116**: 505–524.

Andreoli RV, Kayano MT. 2005. ENSO-related rainfall anomalies in South America and associated circulation features during warm and cold pacific decadal oscillation regimes. *International Journal of Climatology* **25**: 2017–2030.

Andreoli RV, Kayano MT. 2006. Tropical pacific and South Atlantic effects on rainfall variability over Northeastern Brazil. *International Journal of Climatology* DOI: 10.1002/joc.1341.

Barros VR, Silvestri GE. 2002. The relation between sea surface temperature at the subtropical south-central pacific and precipitation in southeastern South America. *Journal of Climate* **15**: 251–267.

Berri GJ, Bertossa GI. 2004. The influence of the tropical and subtropical Atlantic and Pacific Oceans on precipitation variability over southern central South America on seasonal time scales. *International Journal of Climatology* **24**: 415–435.

Brown DJ, Comrie AC. 2004. A winter precipitation 'dipole' in the western United States associated with multidecadal ENSO variability. *Geophysical Research Letters* **31**: L09203, Doi: 10.1029/2003GL018726.

Caviedes CN. 1973. Secas and el niño: two simultaneous climatical hazards in South America. *Proceedings of the Association of American Geographers* **5**: 44–49.

Chelliah M, Bell GD. 2004. Tropical multidecadal and interdecadal climate variability in the NCEP-NCAR reanalysis. *Journal of Climate* **17**: 1777–1803.

Dias de Paiva EMC, Clarke RT. 1995. Time trends in rainfall records in Amazonia. *Bulletin of the American Meteorological Society* **76**: 2203–2209.

Enfield DB, Mestas-Nuñez A. 1999. Multiscale variabilities in global sea surface temperatures and their relationships with tropospheric climate patterns. *Journal of Climate* **12**: 2719–2733.

Garreaud RD, Battisti DS. 1999. Interannual (ENSO) and interdecadal (ENSO-like) variability in the southern hemisphere tropospheric circulation. *Journal of Climate* **12**: 2113–2123.

Garreaud RD, Aceituno P. 2001. Interannual rainfall variability over the South American altiplano. *Journal of Climate* **14**: 2779–2789.

Gershunov A, Barnett TP. 1998. Interdecadal modulation of ENSO teleconnections. *Bulletin of the American Meteorological Society* **79**: 2715–2725.

Giannini A, Saravanan R, Chang P. 2004. The preconditioning role of tropical Atlantic variability in the development of the ENSO teleconnection: implications for the prediction of nordeste rainfall. *Climate Dynamics* **22**: 839–855, Doi: 10.1007/s00382–004–0420–2.

Grimm AM. 2003. The el niño impact on the summer monsoon in Brazil: regional processes versus remote influences. *Journal of Climate* **16**: 263–280.

Grimm AM, Vera CS, Mechoso CR. 2004. The South American monsoon system. World Meteorological Organizations. *The Third International Workshop on Monsoons*, Hangzhou, 2–6 November; 111–129.

Gutzler DS, Kann DM, Thornbrugh C. 2002. Modulation of ENSO-based long-lead outlooks of southwestern U.S. winter precipitation by the pacific decadal oscillation. *Weather Forecasting* **17**: 1163–1172.

Hastenrath S, Heller L. 1977. Dynamics of climatic hazards in northeast Brazil. *Quarterly Journal Royal Meteorological Society* **103**: 77–92.

Hoerling MP, Kumar A, Zhong M. 1997. El niño, la niña, and the nonlinearity of their teleconnections. *Journal of Climate* **10**: 1769–1785.

Hulme MA. 1992. 1951–80 global land precipitation climatology for the evaluation of general circulation models. *Climate Dynamics* **7**: 57–72.

Hulme MA. 1994. Validation of large-scale precipitation fields in general circulation models. In *Global Precipitations and Climate Change*, Desbois M, Desalmand F (eds), NATO ASI series. Springer-Verlag: Berlin; 466.

Hulme MA, Osborn TJ, Johns TC. 1998. Precipitation sensitivity to global warming: comparison of observations with HadCM2 simulations. *Geophysical Research Letters* **25**: 3379–3382.

Kayano MT. 2003. A note on the precipitation anomalies in southern South America associated with ENSO variability in the tropical pacific. *Meteorological and Atmospheric Physics* **84**: 267–274.

Kayano MT, Andreoli RV. 1998. Interanual variability of the upper tropospheric circulation. *Meteorological and Atmospheric Physics* **68**: 143–150.

Kayano MT, Andreoli RV. 2004. Decadal variability of northern northeast Brazil rainfall and its relation to tropical sea surface temperature and global sea level pressure anomalies. *Journal of Geophysical Research* **109**: Doi: 10.1029/2004JC002429 C11011.

Kayano MT, Rao VB, Moura AD. 1988. Tropical circulations and the associated rainfall anomalies during two contrasting years. *Journal Climatology* **8**: 477–488.

Kiladis G, Diaz HF. 1989. Global climatic anomalies associated with extremes in the southern oscillation. *Journal of Climate* **2**: 1069–1090.

Kodama YM. 1992. Large-scale common features of subtropical precipitation zones (the baiu frontal zone, the SPCZ, and the SACZ). Part I: characteristics of subtropical frontal zones. *Journal of the Meteorological Society of Japan* **70**: 813–836.

Kodama YM. 1993. Large-scale common features of subtropical convergence zones (the baiu frontal zone, the SPCZ, and the SACZ). Part II: conditions of the circulations for generating the STCZs. *Journal of the Meteorological Society of Japan* **71**: 581–610.

Kousky VE. 1979. Frontal influences on northeast Brazil. *Monthly Weather Review* **107**: 1140–1153.

Kousky VE, Gan MA. 1981. Upper tropospheric cyclonic vortices in the tropical South Atlantic. *Tellus* **33**: 538–551.

Kousky VE, Ropelewski CF. 1989. Extremes in the southern oscillation and their relationship to precipitation anomalies with emphasis on the South American region. *Revista Brasileira de Meteorologia* **4**: 351–363.

Kousky VE, Kayano MT, Cavalcanti IFA. 1984. A review of the southern oscillation: oceanic-atmospheric circulation changes and related rainfall anomalies. *Tellus* **36A**: 490–504.

Krepper CM, Sequeira ME. 1998. Low frequency variability of rainfall in southeastern South America. *Theoretical and Applied Climatology* **61**: 19–28.

Krishnan R, Sugi M. 2003. Pacific decadal oscillation and variability of the Indian summer monsoon rainfall. *Climate Dynamics* **21**: 233–242.

Mantua NJ, Hare SR, Zhang Y, Wallace JM, Francis RC. 1997. A pacific interdecadal climate oscillation with impacts on salmon production. *Bulletin of the American Meteorological Society* **78**: 1069–1079.

Marengo JA. 2004. Interdecadal variability and trends of rainfall across the amazon basin. *Theoretical and Applied Climatology* **78**: 79–96.

Marengo JA, Tomasella J, Uvo CRB. 1998. Trends in streamflow and rainfall in tropical South America: Amazonia and eastern Brazil, and northwestern Peru. *Journal Geophysical Research* **103**: 1775–1783.

McCabe GJ, Dettinger MD. 1999. Decadal variations in the strength of ENSO teleconnections with precipitation in the western United States. *International Journal of Climatology* **19**: 1399–1410.

Mestas-Nuñez AM, Enfield DB. 2001. Eastern equatorial pacific SST variability: ENSO and non-ENSO components and their climate associations. *Journal of Climate* **14**: 391–402.

Minobe S. 2000. Spatio-temporal structure of the pentadecadal variability over the north pacific. *Progress in Oceanography* **47**: 381–408.

Paegle JN, Mo KC. 2002. Linkages between summer rainfall variability over South America and sea surface temperature anomalies. *Journal of Climate* **15**: 1389–1407.

Panofsky HA, Brier GW. 1968. *Some Applications of Statistics to Meteorology*. Pennsylvania State University; University Park, Pennsylvania 224.

Pezzi LP, Cavalcanti JFA. 2001. The relative importance of ENSO and tropical Atlantic sea surface temperature anomalies for seasonal precipitation over South America: a numerical study. *Climate Dynamics* **17**: 205–212.

Press WH., Flannery BP, Teukolsky SA, Vetterling WT. 1986. *Numerical Recipes: The Art of Scientific Computing*. Cambridge University Press: Cambridge.

Rao VB, Hada K. 1990. Characteristics of rainfall over Brazil: annual and variations and connections with the southern oscillation. *Theoretical and Applied Climatology* **42**: 81–91.

Rao VB, Santo CE, Franchito SH. 2002. A diagnosis of rainfall over South America during the 1997–98 El Niño event. Part I: validation of NCEP-NCAR reanalysis rainfall data. *Journal of Climate* **15**: 502–521.

Rasmusson EM, Arkin PA. 1985. Interannual climate variability associated with the El Niño/southern oscillation. *Coupled Ocean-Atmosphere Models*, Nihoul JCJ (ed.). Elsevier Science Publishers B.V., Amsterdam; 697–725.

Robertson AW, Mechoso CR. 1998. Interannual and decadal cycles in river flows of southeastern South America. *Journal of Climate* **11**: 2570–2581.

Robertson AW, Mechoso CR. 2000. Interannual and interdecadal variability of the South Atlantic convergence zone. *Monthly Weather Review* **128**: 2947–2957.

Ropelewski CF, Halpert MS. 1987. Global and regional scale precipitation patterns associated with the el niño/southern oscillation. *Monthly Weather Review* **115**: 1606–1626.

Ropelewski CF, Halpert MS. 1989. Precipitation patterns associated with the high index phase of the southern oscillation. *Journal of Climate* **2**: 268–284.

Smith TM, Reynolds RW. 2003. Extended reconstruction of global sea surface temperatures based on COADS data (1854–1997). *Journal of Climate* **16**: 1495–1510.

Streten NA. 1973. Some characteristics of satellite-observed bands of persistent cloudiness over the southern hemisphere. *Monthly Weather Review* **101**: 486–495.

Vera C, Silvestri GE, Barros VR, Carril A. 2004. Differences in el niño response over the southern hemisphere. *Journal of Climate* **17**: 1741–1753.

Walker GT. 1928. Ceará (Brazil) famines and the general air movement. *Beiträge zur Physik der Frein Atmosphäre* **14**: 88–93.

Yasunari T. 1977. Stationary waves in the southern hemisphere mid-latitude zone revealed from average brightness charts. *Journal of the Meteorological Society of Japan* **55**: 274–285.

Zhang Y, Wallace JM, Battisti D. 1997. ENSO-like interdecadal variability: 1900–93. *Journal of Climate* **10**: 1004–1020.

Zhang Y, Norris J, Wallace JM. 1998. Seasonality of large-scale atmosphere-ocean interaction over the north pacific. *Journal of Climate* **11**: 2473–2481.

Zhou J, Lau KM. 2001. Principal modes of interannual and decadal variability of summer rainfall over South America. *International Journal of Climatology* **21**: 1623–1644.

DOI: 10.1002/joc